

# Monte Carlo Simulation of Silicon Amorphization During Ion Implantation

Walter Bohmayr, Alexander Burenkov, Jürgen Lorenz, Heiner Ryssel, and Siegfried Selberherr, *Fellow, IEEE*

**Abstract**—We present a new analytical model to predict the spatial location of amorphous phases in ion-implanted single-crystalline silicon using results of multidimensional Monte Carlo simulations. Our approach is based on the concept of the critical damage energy density [1]. Additionally, the self-annealing of radiation damage during ion implantation is taken into account because this effect is crucial for a correct prediction of amorphization. Two aspects of self-annealing are considered, namely, the temperature and the spatial dependence. The latter is related to the local damage energy density, which is simulated by one-, two-, and three-dimensional modules of our Monte Carlo program MCIMPL [2], [3] of the technology CAD framework VISTA [4], [5]. Therefore, the formation and the shape of amorphous regions in single-crystalline silicon can be predicted as a result of Monte Carlo simulations of ion implantation. The suggested model accurately reproduces the results of direct microscopic observations (XTEM measurements) of amorphous layers in silicon after a silicon self-implantation, which are available for a temperature range of 82–296 K [6].

**Index Terms**—Amorphization, implant-induced damage, ion implantation, ion radiation effects, modeling, Monte Carlo methods.

## I. INTRODUCTION

A CONSIDERABLE number of ion-implantation applications in silicon technology require high implantation doses. In these cases, crystalline silicon can be transformed to an amorphous state [7]–[9]. The minimum dose required for amorphization primarily depends on the atomic mass of the ion, the temperature of the substrate, and the ion energy [10]. Usually, a buried amorphous layer appears first at the depth of the maximum radiation damage, and then, the thickness of the amorphous layer grows with increasing implantation dose. The kinetics of recrystallization of amorphous silicon layers is well characterized [11], [12], but the mechanisms of their formation by ion bombardment are still under investigation [13]–[15]. The existence of an amorphous layer leads to a completely different annealing behavior of the radiation defects in silicon.

Manuscript received February 24, 1997; revised May 11, 1998. This work was supported in part by the European Commission under ESPRIT project 8150 and in part by PROMPT under JESSI project BT8B. This paper was recommended by Associate Editor Z. Yu.

W. Bohmayr is with ISE Integrated Systems Engineering AG, Zurich CH-8005 Switzerland (e-mail: bohmayr@ise.ch).

A. Burenkov and J. Lorenz are with the Device Technology Division, Fraunhofer Institute of Integrated Circuits, Erlangen D-91058 Germany.

H. Ryssel is with the Device Technology Division, Fraunhofer Institute of Integrated Circuits, Erlangen D-91058 Germany and the Department of Electrical Engineering, University of Erlangen-Nuremberg, Germany.

S. Selberherr is with the Institute for Microelectronics, Vienna University of Technology, Vienna A-1040 Austria.

Publisher Item Identifier S 0278-0070(98)09359-2.

In particular, amorphous layers recrystallize by solid-phase epitaxy during a postimplantation high-temperature treatment. Under certain conditions, these recrystallized layers are found to be practically defect free [11], [16]. In other words, the type and amount of the remaining defects in silicon after an annealing step crucially depends on the size and location of the amorphous layer [17]–[20]. Therefore, a detailed knowledge of the properties of postimplantation defects is an important requirement for a predictive simulation of transient enhanced diffusion (TED) observed during rapid thermal annealing (RTA). TED caused by postimplantation defects is also a possible explanation of the reverse short channel effect (RSCE) in MOSFET's [21].

## II. GOALS AND ASSUMPTIONS

As a first step toward the simulation of extended defects remaining after implantation and annealing, we have developed a model to simulate amorphization of single-crystalline silicon using a Monte Carlo method. The critical parameters ruling the amorphization process are the implantation dose  $D$ , the ion mass, the ion energy  $E_{\text{ion}}$ , and the substrate temperature  $T$ . Our goal was the extension of the Monte Carlo code MCIMPL [2], [3] of the technology CAD (TCAD) framework VISTA [4], [5] in order to be able to predict the formation of amorphous regions during ion implantation and their spatial location. It should be mentioned that MCIMPL also considers channeling phenomena of ions in crystalline silicon [22].

The approach is based on the critical damage energy density (CED) model [1], which assumes that the transformation to the amorphous state happens when the energy deposited in nuclear collisions by ions and recoil atoms exceeds a critical threshold. The major problem in simulation of amorphization processes is the self-annealing of radiation damage during ion implantation even at low temperatures. Therefore, Morehead *et al.* [23], [24] adapted the original CED model for description of the temperature-dependent amorphization, and additionally, Maszara and Rozgonyi experimentally showed in [6] that self-annealing also depends on the depth of the amorphous-crystalline (a/c) interfaces.

The task of this work was to develop an analytical amorphization model for binary collision TCAD codes that accounts for substrate temperature effects and includes the experimentally observed depth dependence of self-annealing. To calibrate our model, we have studied experimental results.

As mentioned above, the damage energy density  $e_d$  is of crucial importance to our model. We define  $e_d$  as the energy deposited in nuclear collisions by ions and recoil atoms. In the

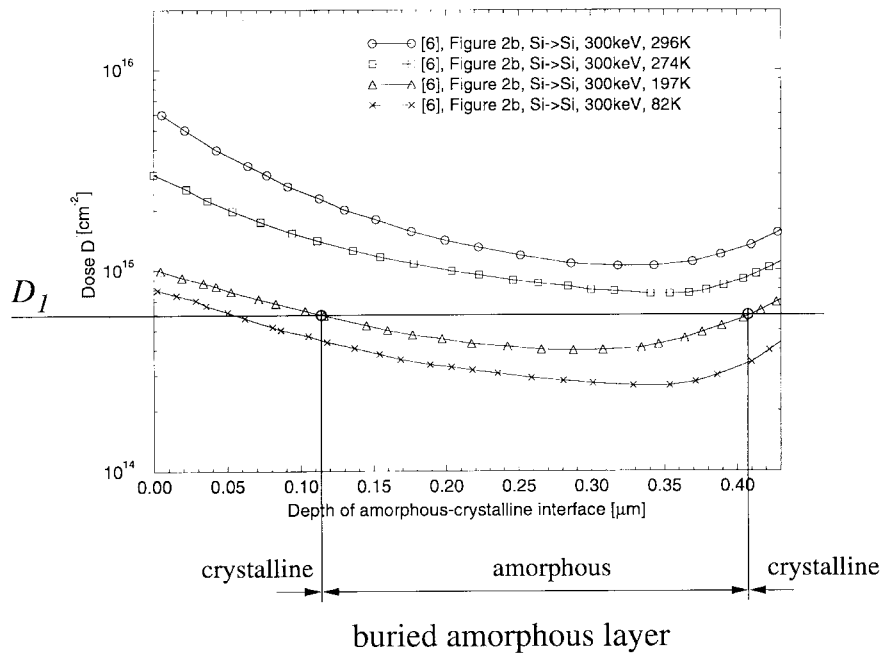


Fig. 1. The depths of amorphous-crystalline interfaces, as measured from XTEM micrographs, as a function of  $^{28}\text{Si}^+$  dose at 300 keV. The substrate temperature ranges from 82 to 296 K.

present study, we apply a modified Kinchin–Pease model [25], [26] to calculate  $c_d$  because a well-known advantage of such a strategy is its much lower demand for computer resources in comparison with simulations of all recoil trajectories. On the other hand, it is also evident that the kinetic energy that is transferred by the ions in elastic processes dissipates due to the development of collision cascades. As demonstrated in [27] and [28], this knock-on transport is negligible during implantation of light- and medium-mass ions. For heavy ions like arsenic and antimony, however, one should contemplate this kind of energy transport (see Section V-A).

### III. EXPERIMENTAL DATA

We evaluated a number of experimental results [6], [19], [29], [30], [23], [24], [31]–[35]. Especially, the work of Maszara and Rozgonyi [6] contains a detailed analysis of silicon self-implantation experiments under well-defined conditions. Based on their well-substantiated results, we calibrated our amorphization model for Monte Carlo simulators. Maszara and Rozgonyi implanted p-type (100) silicon wafers with  $^{28}\text{Si}^+$  at two different energies, 150 and 300 keV, with doses ranging from  $2 \cdot 10^{14}$  to  $1 \cdot 10^{16}$   $\text{cm}^{-2}$  at a dose rate of  $0.25 \mu\text{A}\cdot\text{cm}^{-2}$ . The sample holder of the implanter was cooled by liquid nitrogen ( $T_{\text{LN}}$ ), dry ice and acetone, ice and water, and water at room temperature ( $T_{\text{RT}}$ ) to maintain sample temperatures of 82, 197, 274, and 296 K, respectively.

They measured the damage structure of implanted samples using cross-section transmission electron microscopy (XTEM) technique. If an amorphous layer was formed by ion bombardment, its thickness was directly measured from XTEM micrographs [6], considering only continuous amorphous regions containing no visible detached microcrystallites.

#### A. Dose for Amorphization Obtained from XTEM Micrographs

Fig. 1 depicts the relation between the implantation dose  $D$  of  $^{28}\text{Si}^+$  at 300 keV and the depths of a/c-interfaces, as measured from XTEM micrographs. The curves, in the following called the dose-depth relations, are shown for a number of substrate temperatures  $T$  (82, 197, 274, and 296 K). For example, if we implant  $^{28}\text{Si}^+$  at 300 keV with a dose of  $D_1 = 6 \cdot 10^{14}$   $\text{cm}^{-2}$  at a temperature of 197 K, silicon is amorphized between 0.11 and 0.41  $\mu\text{m}$  (see Fig. 1). The area above this U-shaped dose-depth relation corresponds to amorphous material, and that lying below of it represents crystalline matter. In other words, the curves indicate the threshold values of dose for which the sample becomes amorphous at a given depth.

Important properties of the amorphization process can be derived from Fig. 1.

- Each curve shows a more or less pronounced minimum indicating a critical amorphization dose  $D_c$ . If the implantation dose  $D$  is below  $D_c$  at a given temperature  $T$ , no amorphization takes place.
- Amorphization during ion implantation at elevated temperatures requires a higher critical amorphization dose  $D_c$ .
- An amorphous layer is formed if  $D \geq D_c$  and its thickness grows with increasing  $D$ . In this case, we talk about amorphization doses  $D_a$ , in contrast to the critical amorphization dose  $D_c$ .
- The minima of the dose-depth relations for different temperatures are located at almost the same depths, which are close to the depth of the maximum radiation damage.

### B. Critical Amorphization Energy Density $e_c$

The damage energy density  $e_d$  in eV/atom can be defined as follows:

$$e_d(x) = \frac{D}{N_{\text{Si}}} \cdot \frac{dE_d(x)}{dx} \quad (1)$$

where  $D$  denotes the implantation dose,  $N_{\text{Si}}$  is the atomic density of silicon ( $5 \cdot 10^{22} \text{ cm}^{-3}$ ), and  $dE_d(x)/dx$  is the nuclear energy loss per unit depth at a depth  $x$ . Ions as well as silicon recoils within the collision cascade contribute to  $e_d$ . Since the nuclear energy loss  $E_d$  for each atomic collision is calculated by the Monte Carlo simulator, we can easily derive  $e_d$  even for the three-dimensional case.

According to the CED model, amorphization at a point  $\vec{r}$  happens if  $e_d$  exceeds a critical threshold  $e_c$

$$e_d(\vec{r}) \geq e_c(T, \vec{r}). \quad (2)$$

$e_c(T, \vec{r})$  is the critical damage energy density to render crystalline silicon amorphous at a substrate temperature  $T$  and at spatial location  $\vec{r}$ .

### C. Experimental Verification of the Calculated Damage Energy Density $e_d$

The calculated profiles of damage energy deposition can be verified experimentally under the assumption that at very low substrate temperatures ( $T \leq T_{\text{LN}}$ ), any significant annealing of the radiation damage is prevented, and there is virtually no migration of point defects. Thus, the transition to an amorphous phase at extreme low temperatures requires the deposition of the same amount of  $e_c = e_{c,0}$  regardless of its location. The lack of dose rate effects at  $T_{\text{LN}}$  [36] and investigations using Raman spectroscopy together with XTEM [32] supports these suppositions. The critical damage energy density at very low temperatures  $e_{c,0}$  was found to be equal to 12 eV/atom ( $6 \cdot 10^{23} \text{ eV/cm}^3$ ) [6], [37], [38] independent of implantation energies (see Section III-D).

Assuming a constant critical energy density at low temperatures  $e_{c,0}$  in eV/atom, we can easily derive experimental profiles of damage energy deposition from the results of the XTEM measurements

$$\frac{dE_d(x)^{\text{exp}}}{dx} = \frac{e_{c,0} \cdot N_{\text{Si}}}{D_a(x)} \quad (3)$$

where  $D_a(x)$  represents the dose for amorphization at the depth  $x$ . Fig. 2 depicts the comparison of experimental (symbols) and simulated profiles of damage energy deposition. The depths of the peaks  $R_d$  of the experimentally derived  $dE_d(x)/dx$  profiles are in excellent agreement with the simulated ones. A noticeable deviation between the curves near the surface of the sample is observed. A possible explanation can be a loss of point defects to the surface, which is an unsaturable sink for such defects [39].

### D. Temperature-Dependent Effects

Implanted ions dissipate part of their kinetic energy in elastic collisions with the substrate atoms. This process is terminated after about a few tenths of a picosecond. During

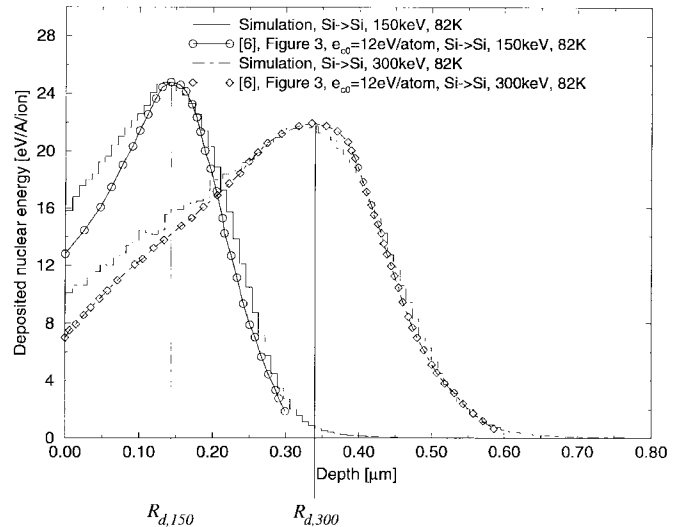


Fig. 2. Comparison of experimental (symbols) and simulated profiles of damage energy deposition (eV/Å/Ion). The experimental result of Fig. 1 at  $T_{\text{LN}}$  and (3) were used to obtain the experimental plot.

the next nanoseconds or so [30], a thermalization process causes part of the atomic cascade to become annihilated due to interaction among moving point defects. Of course, the most important boundary condition for self-annealing is the substrate temperature. Three different temperature ranges of the thermally assisted cascade collapsing can be determined as illustrated in Fig. 3. These curves represent the critical energy densities  $e_c$  measured by Maszara and Rozgonyi [6].

- 1) At elevated temperatures ( $T \approx 250 \text{ K}$  and higher), a “cigar-shaped” damage cascade radially collapses into an amorphous one of smaller radius due to thermally assisted vacancy out-diffusion from the cascade center [6], [23], [40] (self-annealing). The upward bending of the curves left and right of  $R_d$  points to a higher probability of damage self-annealing at the cascade periphery. We relate this phenomenon to the actual distribution of damage within the cascade. Less densely distributed vacancies (see Fig. 2) will be more prone to dynamic annealing before they are able to form stable damage.
- 2) At lower temperatures ( $T \approx 200 \text{ K}$ ),  $e_c$  is independent of the depth. However, a small part of the radiation damage is self-annealed, and the probability for this process is independent of the cascade density.
- 3) At very low temperatures ( $T \leq T_{\text{LN}}$ ), any appreciable annealing of unstable defects is prevented as mentioned above, and the assumption of a constant critical energy density  $e_{c,0}$  holds.

## IV. IMPLEMENTATION OF THE AMORPHIZATION MODEL

The fundamental idea of our approach is to separate the problem of damage self-annealing into two parts.

- 1) *Temperature-dependent part*: We use an analytical out-diffusion model [6], [23], [40], which describes the radial collapse of the damage cascade depending on the implantation temperature.

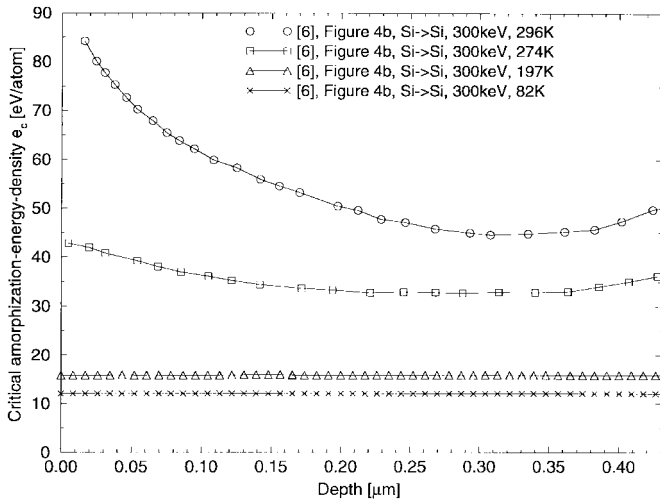


Fig. 3. Critical amorphization energy density  $e_c$  as a function of depth for several temperatures and an implantation energy of 300 keV. The upward bending of the curves indicates that the rate of the thermally assisted cascade collapsing is a function of depth.

2) *Depth-dependent part:* We associate the depth dependencies with the deposited damage energy density  $e_d(\vec{r})$ . In fact,  $e_d$  is a measure for the cascade density, and areas with a lower density are assumed to anneal easier at a certain temperature compared to stronger damaged regions, as indicated by experimental observations [6], [34].

#### A. Out-Diffusion Model for Considering Temperature Dependence: $e_c = f(T)$

Following the experimental results of Maszara and Rozgonyi [6], we apply the model of Morehead and Crowder [23] to describe the temperature-dependent amorphization. They derived the following relation between  $e_c$  and  $T$ , valid for  $T \leq T_{\text{inf}}$ :

$$e_c(T) = e_{c,0} \cdot \left(1 - \exp\left(\frac{E_{\text{act}} \cdot (T - T_{\text{inf}})}{2kT \cdot T_{\text{inf}}}\right)\right)^{-2}. \quad (4)$$

$E_{\text{act}}$  represents the activation energy of vacancy out-diffusion,  $T_{\text{inf}}$  reflects that temperature above which no amorphization can occur, and  $k$  is Boltzmann's constant. Experiments in [6] proved that at depths of stronger damage,  $E_{\text{act}}$  decreases and  $T_{\text{inf}}$  increases.

To quantify the general temperature dependence (4), we extract the model parameters  $E_{\text{act}}$  and  $T_{\text{inf}}$  for boron, silicon, phosphorus, and arsenic ions by fitting the known temperature dependence of  $D_c$  for these ions [6], [10]. As mentioned above, the onset of amorphization happens at the depth of the maximum damage, and thus, this procedure ensures a reliable reproduction of experimental results, especially at implantation doses close to  $D_c$ .

Fig. 4 compares experimental (symbols) with theoretical results of  $e_c(T)$  at the depth of the maximum damage. Thus, for the latter one, we apply (4) at  $R_d$ . The model parameters  $T_{\text{inf}}$  and  $E_{\text{act}}$  at this particular depth are denoted as  $\hat{T}_{\text{inf}}$  and  $\hat{E}_{\text{act}}$ . An important result is the fact that the 150-keV ion beam requires *lower* threshold energy densities than the 300-keV

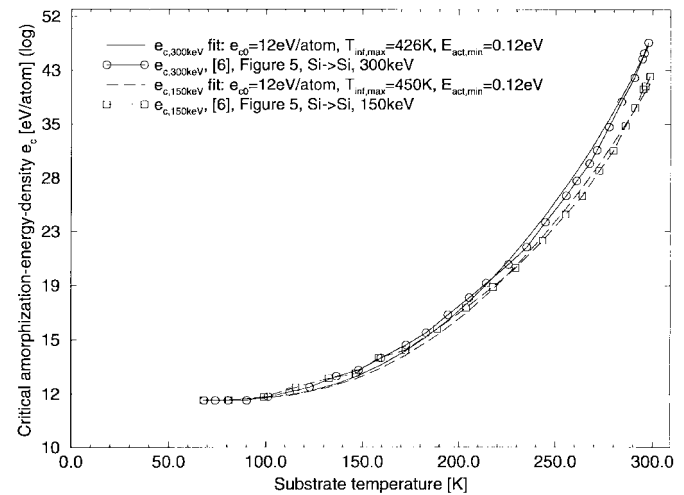


Fig. 4. Critical amorphization energy density  $e_c$  as a function of substrate temperature  $T$  for silicon self-implantation at energies of 150 and 300 keV (semilogarithmic representation). The experimental data (symbols) correspond to those  $e_c$  values of Fig. 3 at the depth of the damage peak  $R_d$ . As the graphs depict, the amorphization by the 150-keV ion beam requires *lower* threshold energy densities, indicating better stability of damage against self-annealing.

TABLE I  
THE PARAMETERS  $\hat{E}_{\text{act}}$  AND  $\hat{T}_{\text{inf}}$  OF THE OUT-DIFFUSION MODEL DERIVED FROM EXPERIMENTS [6], [10]

| Ion | $E_{\text{ion}}$ [keV] | $\hat{E}_{\text{act}}$ [meV] | $\hat{T}_{\text{inf}}$ [K] |
|-----|------------------------|------------------------------|----------------------------|
| B   | 200                    | 77                           | 305                        |
| Si  | 300                    | 120                          | 426                        |
| P   | 40                     | 90                           | 437                        |
| As  | 40                     | 120                          | 600                        |

one, indicating better stability of the damage against self-annealing at 150 keV. Again, the profiles of damage energy deposition (Fig. 2) depict  $\hat{e}_{d,150} > \hat{e}_{d,300}$ , in agreement with the assumption of easier amorphization in regions with higher  $e_d$ . This observation supports the idea to model the spatial dependence of  $e_c$  by  $e_d$ . Table I gives the values for  $\hat{E}_{\text{act}}$  and  $\hat{T}_{\text{inf}}$  derived from experimental data [6], [10].

#### B. Modeling of the Spatial Dependence: $e_c = f(\vec{r})$

As shown above,  $E_{\text{act}}$  and  $T_{\text{inf}}$  describe the temperature dependence of  $e_c$ . The model (4) depicted in Fig. 4 is calibrated at the depth of the maximum damage  $R_d$ . To consider the depth dependence, we apply this equation at other points and determine the corresponding values of  $T_{\text{inf}}$  and  $E_{\text{act}}$  from experiments. As anticipated,  $T_{\text{inf}}$  steadily increases with increasing damage density deposited by an ion [6], i.e., more stable damage is created in heavier damaged regions.

On the other hand,  $E_{\text{act}}$  steadily decreases with increasing density of the collision cascade [6], indicating an enhancement of diffusion of individual vacancies in stronger damaged regions.

Taking  $e_d$  as a measure for the cascade density and using experimental data [6] on local self-annealing, we derive the following fitting functions of  $e_d$  to describe the spatial de-

TABLE II  
THE PARAMETERS  $p_T$  AND  $p_E$  FOR MODELING THE SPATIAL  
DEPENDENCE OF  $e_c$  DERIVED FROM EXPERIMENTS [6]

| Ion | $p_T$ | $p_E$ |
|-----|-------|-------|
| Si  | 0.31  | 0.63  |

pendence of damage self-annealing for the first time with an analytical model:

$$T_{\text{inf}}(\vec{r}) = \hat{T}_{\text{inf}} \cdot \left( \frac{e_d(\vec{r})}{\hat{e}_d} \right)^{p_T} \quad (5)$$

$$E_{\text{act}}(\vec{r}) = \min\left(0.20 \text{ eV}, \hat{E}_{\text{act}} \cdot \left( \frac{\hat{e}_d}{e_d(\vec{r})} \right)^{p_E}\right) \quad (6)$$

where  $\hat{e}_d$  is the maximum damage energy density at  $R_d$  and the parameters  $p_T$  and  $p_E$  determine the spatial dependence of  $T_{\text{inf}}(\vec{r})$  and  $E_{\text{act}}(\vec{r})$  according to the experimental data. A value of 0.20 eV for the maximum of the activation energy  $E_{\text{act}}$  is assumed. Dennis and Hale [14] obtained this value during investigations of ion-implanted silicon, and they associated it with the migration of double-negative-charged vacancies in undamaged silicon.

Further analysis of experimental results [6], [14] showed that  $\hat{E}_{\text{act}}$ ,  $p_T$ , and  $p_E$  only slightly depend on  $E_{\text{ion}}$  [14] and that  $\hat{T}_{\text{inf}}$  for silicon self-implantation can be scaled by

$$\frac{\hat{T}_{\text{inf},150 \text{ keV}}}{\hat{T}_{\text{inf},300 \text{ keV}}} = \left( \frac{\hat{e}_{d,150 \text{ keV}}}{\hat{e}_{d,300 \text{ keV}}} \right)^{p_T}. \quad (7)$$

To verify (7), we calculated the expression on the left-hand side using experimental data [6] and evaluated the expression on the right-hand side using Monte Carlo results. Table II gives the values for  $p_E$  and  $p_T$  derived from [6].

### C. Validity of the Amorphization Model for Other Dopants

The presented amorphization model relies on three basic assumptions.

- 1) Correctness of the spatial distribution of  $e_d$ , which is calculated by the Monte Carlo program.
- 2) Validity of the analytical model describing the temperature as well as the depth dependence of  $e_c$ .
- 3) Validity of the CED concept for given implantation conditions.

The first assumption was justified in Section III-C. The temperature dependence of the critical amorphization dose  $D_c$  measured for common doping impurities (boron, phosphorus, and arsenic) and silicon self-implantation was used to find the model parameters  $\hat{T}_{\text{inf}}$  and  $\hat{e}_{\text{act}}$  for the damage self-annealing in the center of the cascade (see Table I). However, the values of the model parameters  $p_T$  and  $p_E$  of (5) and (6), which describe the spatial dependence of damage self-annealing in our model, were obtained from silicon self-implantation experiments (see Table II). In fact, the cascade density strongly depends on the ion mass [1], [17], [33], [42]–[46], and therefore, parameters  $p_T$  and  $p_E$  may deviate from the given values. In other words,  $p_T$  and  $p_E$  of (5) and (6) are only valid in a not-too-wide range of cascade densities.

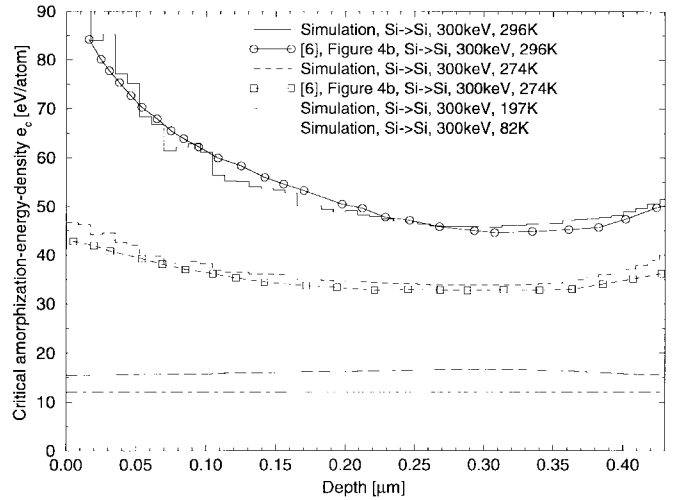


Fig. 5. Comparison between experimental (symbols) and simulated critical amorphization energy density  $e_c$  in eV/atom.

It should be mentioned that collisions between silicon atoms considerably contribute to the damage production within a collision cascade. Therefore, we anticipate that our model parameters  $p_T$  and  $p_E$  calibrated for silicon self-implantation can be applied to other ion species as a first approximation. Furthermore, to obtain correct results, the proposed approach must only be precise for a relatively narrow range of  $e_d$  (see Fig. 3).

Summing up, the damage energy density  $e_d$  can be accurately calculated by MCIMPL for boron, silicon, phosphorus, and arsenic at least within a range that is relevant for amorphization processes. The temperature dependence of  $D_c$  is excellently reproduced by the suggested model (see Fig. 4). The combined effect of temperature and spatial dependence of damage self-annealing is justified for ions with medium atomic mass (silicon and phosphorus). Additional calibrations are required to obtain reliable predictions of damage self-annealing if heavier ions are implanted with doses much higher than the critical ones. The spatial dependence of  $e_c$  is one of the key points to describe the development of the amorphous layers when the dose is increased over  $D_c$ . Models neglecting this dependence would predict thicker amorphous layers compared to experimental results.

## V. SIMULATION RESULTS

To verify our approach, we present two implantation simulations with:

- ion:  $^{28}\text{Si}^+$ ;
- $E_{\text{ion}}$ : 150 keV, 300 keV;
- $D$ :  $3 \cdot 10^{14} \text{ cm}^{-2}$ ;
- implantation window: 1  $\mu\text{m}$ ;
- (100) single-crystalline silicon wafer;
- wafer tilted by  $7^\circ$  from [100] direction.

With  $e_d(\vec{r})$  calculated by the Monte Carlo simulator and self-annealing effects taken into account by (4)–(7), we calculated the critical amorphization energy density  $e_c(T, \vec{r})$ .

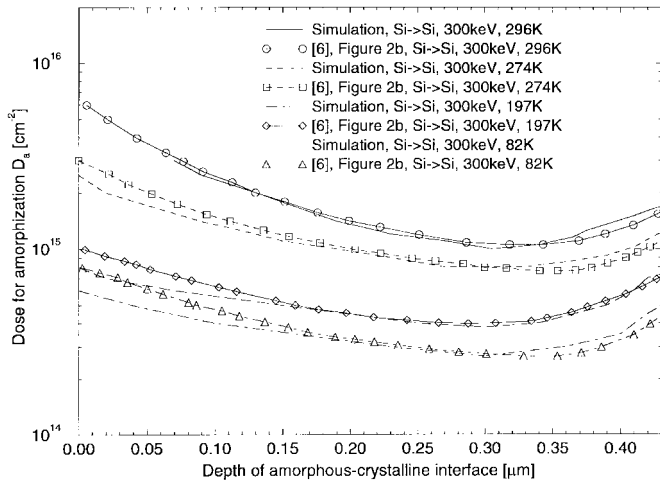


Fig. 6. Comparison between experimental (symbols) and simulated dose for amorphization  $D_a$  versus depths of amorphous-crystalline interfaces.

Fig. 5 shows the excellent agreement of our Monte Carlo simulations with the experimental results (symbols). A depth independence of  $e_c$  is only predicted at  $T \leq 197$  K.

Since the influence of the thermal vibrations of the silicon atoms [47] is negligible for the distribution of the damage energy density,  $e_d$  is practically independent of  $T$  and proportional to  $D$ . Therefore, we can calculate the dose for amorphization  $D_a$  with  $e_c(T, \vec{r})$  and (1) and (2) assuming the critical case  $e_d(\vec{r}) = e_c(T, \vec{r})$ .

Fig. 6 depicts that our model is able to reproduce the experimental results in [6], which exhibit depth-dependent self-annealing effects.

#### A. Application Example: Arsenic Implantation

To demonstrate the applicability of our new simulation feature in two-dimensional simulations, we performed a drain implantation simulation of an NMOS device with  $^{33}\text{As}^+$ , 60 keV,  $5 \cdot 10^{15} \text{ cm}^{-2}$ , tilted by  $7^\circ$  from [100] direction, and twisted around the  $y$ -axis by  $90^\circ$ .

The simulation area (Fig. 7) includes a (100) silicon substrate, a thin gate oxide of 10 nm, and the polysilicon gate. The slope of the gate is approximately  $85^\circ$ . The two-dimensional doping distribution of arsenic shows a small lateral penetration under the gate, which is the result of the large atomic mass of arsenic in comparison to silicon.

A continuous amorphous layer is predicted by our model after the drain implant (Fig. 8), and the lateral extension of this layer is comparable with the lateral extension of a doping isoline at  $1 \cdot 10^{19} \text{ cm}^{-3}$ . Some of the implantation damage outside the amorphized region may survive the recrystallization step. Such postimplantation defects, in particular the retrograde profile of silicon interstitials in the channel region, are a possible source for the RSCE [21]. The predicted depth of the amorphization layer ( $92 \pm 3$  nm) is in excellent agreement with the results of experimental measurements [48] (94 nm).

As already mentioned in Section II, the recoil transport during implantation of heavy ions widens the distribution of the damage energy density  $e_d$ . Therefore, we simulated the full

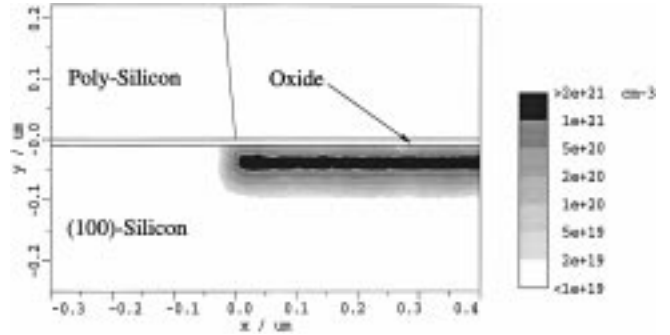


Fig. 7. As-implanted profile in silicon of a typical two-dimensional technology-related example at  $T = 296$  K:  $^{33}\text{As}^+$  ions, 60 keV,  $5 \cdot 10^{15} \text{ cm}^{-2}$ , tilted by  $7^\circ$  from [100] direction, and twisted around the  $y$ -axis by  $90^\circ$ .

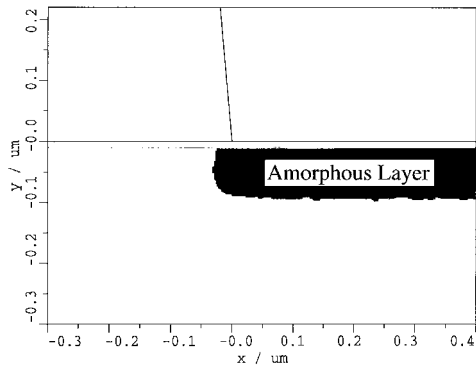


Fig. 8. Resulting amorphous layer of our two-dimensional example calculated at  $T = 296$  K. The simulation result corresponds to experimental data [48] very well.

collision cascades to determine  $e_d$  produced by the arsenic ions.

## VI. CONCLUSION

A new amorphization model for Monte Carlo simulation of ion implantation that is applicable to arbitrary one-, two-, and three-dimensional geometries is presented. Using results of silicon self-implantation experiments, we have derived a physically based strategy to predict amorphous layers in ion-implanted single-crystalline silicon. The approach is based on the critical damage energy density model, which assumes that the transformation to the amorphous state happens when the energy deposited in nuclear collisions by ions and recoils exceeds a critical threshold  $e_c(T, \vec{r})$ . The dynamic annealing of the damage during ion implantation is separated into two parts: 1) a temperature-dependent part and 2) a spatially dependent part. We couple both subproblems by assuming that parameters of the temperature-dependent out-diffusion model are local functions of the deposited damage energy density  $e_d$ . In fact,  $e_d$  is a measure for the collision cascade density, and areas with less densely distributed radiation defects will be more prone to self-annealing before they are able to form stable damage.

Almost no additional CPU time is required by our model, and the implementation into existing codes is straightforward. The critical parameters ruling the amorphization process are the substrate temperature, the implantation dose, the implanta-

tion energy, and the ion mass, which are all taken into account by our approach.

Our simulations depict that the approach outlined above has potential for further optimization and refinement. Especially, investigation of ion species and dose rate effects [49], [50] could contribute to better calibrations, which are required for predictive simulations of TED effects.

#### ACKNOWLEDGMENT

The authors would like to thank A. Hössinger for helpful discussions and for performing MCIMPL simulations that consider knock-on transport. W. Bohmayr wishes to acknowledge that part of this work was performed during his SUSTAIN fellowship at the Fraunhofer Institute of Integrated Circuits, Device Technology Division, Erlangen, Germany.

#### REFERENCES

- [1] F. L. Vook, "Radiation damage during ion implantation in silicon," in *Radiation Damage and Defects in Semiconductors*, J. E. Whitehouse, Ed. London, U.K.: Institute of Physics, 1973, pp. 60–71.
- [2] W. Bohmayr, A. Burenkov, J. Lorenz, H. Ryssel, and S. Selberherr, "Trajectory split method for Monte Carlo simulation of ion implantation," *IEEE Trans. Semiconduct. Manufact.*, vol. 8, no. 4, pp. 402–407, 1995.
- [3] W. Bohmayr, A. Burenkov, J. Lorenz, H. Ryssel, and S. Selberherr, "Statistical accuracy and CPU time characteristic of three trajectory split methods for Monte Carlo simulation of ion implantation," in *Simulation of Semiconductor Devices and Processes*, H. Ryssel and P. Pichler, Eds. Wien, Austria: Springer, 1995, vol. 6, pp. 492–495.
- [4] S. Halama, C. Pichler, G. Rieger, G. Schrom, T. Simlinger, and S. Selberherr, "VISTA—User interface, task level, and tool integration," *IEEE Trans. Computer-Aided Design*, vol. 14, no. 10, pp. 1208–1222, 1995.
- [5] S. Halama, F. Fasching, C. Fischer, H. Kosina, E. Leitner, P. Lindorfer, C. Pichler, H. Pimingstorfer, H. Puchner, G. Rieger, G. Schrom, T. Simlinger, M. Stiftinger, H. Stippel, E. Strasser, W. Tuppa, K. Wimmer, and S. Selberherr, "The Viennese integrated system for technology CAD applications," *Microelectron. J.*, vol. 26, nos. 2/3, pp. 137–158, 1995.
- [6] W. P. Maszara and G. A. Rozgonyi, "Kinetics of damage production in silicon during self-implantation," *J. Appl. Phys.*, vol. 60, no. 7, pp. 2310–2315, 1986.
- [7] G. Dearnaley, J. H. Freeman, R. S. Nelson, and J. Stephen, *Ion Implantation*, vol. 8 of *Defects in Crystalline Solids*. Amsterdam, The Netherlands: North-Holland, 1973.
- [8] A. G. Cullis and D. C. Joy, Eds., *Microscopy of Semiconducting Materials 1981*, vol. 60 of *Institute of Physics Conference Series*. Bristol, U.K.: Adam Hilger, 1981.
- [9] J. Narayan and T. Y. Tan, Eds., *Defects in Semiconductors*, vol. 2 of *Material Research Society Symposia Proceedings*. New York: North-Holland, 1981.
- [10] H. Ryssel and I. Ruge, *Ion Implantation*. New York: Wiley, 1986.
- [11] G. L. Olson and J. A. Roth, "Kinetics of solid phase crystallization in amorphous silicon," *Mater. Sci. Rep.*, vol. 3, no. 1, pp. 1–78, 1988.
- [12] S. Roorda, W. C. Sinke, J. M. Poate, and D. C. Jacobson, "Structural relaxation and defect annihilation in pure amorphous silicon," *Phys. Rev. B*, vol. 44, no. 8, pp. 3702–3725, 1991.
- [13] O. W. Holland, S. J. Pennycook, and G. L. Albert, "New model for damage accumulation in Si during self-ion irradiation," *Appl. Phys. Lett.*, vol. 55, no. 24, pp. 2503–2505, 1989.
- [14] S. U. Campisano, S. Coffa, V. Raineri, F. Priola, and E. Rimini, "Mechanisms of amorphization in ion implanted crystalline silicon," *Nucl. Instr. Meth. B*, vols. 80/81, pp. 514–518, 1993.
- [15] T. Motooka, "Atomistic simulations of amorphization processes in ion-implanted Si: Roles of defects during amorphization, relaxation, and crystallization," *Thin Solid Films*, vol. 272, no. 2, pp. 235–243, 1996.
- [16] T. E. Seidel and A. U. MacRae, "The isothermal annealing of boron implanted silicon," *Rad. Eff.*, vol. 7, nos. 1–2, pp. 1–6, 1971.
- [17] K. S. Jones, S. Prussin, and E. R. Weber, "A systematic analysis of defects in ion-implanted silicon," *Appl. Phys. A*, vol. 45, pp. 1–34, 1988.
- [18] R. J. Schreutelkamp, J. S. Custer, J. R. Liefting, W. X. Lu, and F. W. Saris, "Pre-amorphization damage in ion-implanted silicon," *Mat. Sci. Rep.*, vol. 6, nos. 7/8, pp. 275–366, 1991.
- [19] B. El-Kareh, *Fundamentals of Semiconductor Processing Technologies*. Boston, MA: Kluwer, 1995.
- [20] E. Rimini, *Ion Implantation: Basics to Device Fabrication*. Boston, MA: Kluwer, 1995.
- [21] C. S. Rafferty, H.-H. Vuong, S. A. Eshraghi, M. D. Giles, M. R. Pinto, and S. J. Hillenius, "Explanation of reverse short channel effect by defect gradients," in *Proc. Int. Electron Devices Meeting*, 1993, pp. 311–314.
- [22] G. Hobler and H. W. Pötzl, "Electronic stopping of channeled ions in silicon," in *Proc. Mat. Res. Soc. Symp.*, 1993, vol. 279, pp. 165–170.
- [23] F. F. Morehead, Jr., and B. L. Crowder, "A model for the formation of amorphous Si by ion bombardment," *Rad. Eff.*, vol. 6, pp. 27–32, 1970.
- [24] F. F. Morehead, B. L. Crowder, and R. S. Title, "Formation of amorphous silicon by ion bombardment as a function of ion, temperature, and dose," *J. Appl. Phys.*, vol. 43, no. 3, pp. 1112–1118, 1972.
- [25] G. H. Kinchin and R. S. Pease, "The displacement of atoms in solids by radiation," *Rep. Progress Phys.*, vol. 18, pp. 1–51, 1955.
- [26] M. J. Norgett, M. T. Robinson, and I. M. Torrens, "A proposed method of calculating displacement dose rates," *Nucl. Eng. Des.*, vol. 33, pp. 50–54, 1975.
- [27] G. Hobler, "Simulation der Ionenimplantation in ein-, zwei- und Dreidimensionalen Strukturen," doctoral dissertation, Technische Universität Wien, Austria, Nov. 1988.
- [28] A. Simionescu, S. Herzog, G. Hobler, R. Schork, J. Lorenz, C. Tian, and G. Stinger, "Modeling of electronic stopping and damage accumulation during arsenic implantation in silicon," *Nucl. Instr. Meth. B*, vol. 100, pp. 483–489, 1995.
- [29] J. E. Westmoreland, J. W. Mayer, F. H. Eisen, and B. Welch, "Production and annealing of lattice disorder in silicon by 200-keV boron ions," *Appl. Phys. Lett.*, vol. 15, no. 9, pp. 308–310, 1969.
- [30] J. W. Mayer, L. Eriksson, and J. A. Davies, *Ion Implantation in Semiconductors*. New York: Academic, 1970.
- [31] T. Motooka and O. W. Holland, "Amorphization processes in self-ion-implanted Si: Dose dependence," *Appl. Phys. Lett.*, vol. 58, no. 21, pp. 2360–2362, 1991.
- [32] T. Motooka, F. Kobayashi, P. Fons, T. Tokuyama, T. Suzuki, and N. Natsuaki, "Amorphization processes in ion implanted Si: Temperature dependence," *Jpn. J. Appl. Phys.*, vol. 30, no. 12B, pp. 3617–3620, 1991.
- [33] T. Motooka and O. W. Holland, "Amorphization processes in ion implanted Si: Ion species effects," *Appl. Phys. Lett.*, vol. 61, no. 25, pp. 3005–3007, 1992.
- [34] T. Hara, T. Muraki, M. Sakurai, S. Takeda, M. Inoue, and S. Fujii, "Damage depth profiles for high energy ion implanted silicon," *Nucl. Instr. Meth. B*, vol. 74, pp. 191–196, 1993.
- [35] Q.-T. Zhao, Z.-L. Wang, T.-B. Xu, P.-R. Zhu, J.-S. Zhou, X.-D. Liu, J.-T. Liu, and K.-M. Wang, "Damage formation in Si(100) induced by MeV self-ion implantation," *Nucl. Instr. Meth. B*, vol. 82, pp. 575–578, 1993.
- [36] O. W. Holland, D. Fathy, and J. Narayan, "Damage nucleation in Si during ion irradiation," in *Advanced Photon and Particle Techniques for the Characterization of Defects in Solids*, J. B. Roberto, R. W. Carpenter, and M. C. Wittels, Eds., *Proc. Mat. Res. Soc. Symp.*, 1985, vol. 41, pp. 307–312.
- [37] J. Narayan, D. Fathy, O. S. Oen, and O. W. Holland, "Atomic structure of ion implantation damage and process of amorphization in semiconductors," *J. Vac. Sci. Technol. A*, vol. 2, no. 3, pp. 1303–1308, 1984.
- [38] H. J. Stein, F. L. Vook, D. K. Brice, J. A. Borders, and S. T. Picraux, "Infrared studies of the crystallinity of ion-implanted Si," *Rad. Eff.*, vol. 6, nos. 1–2, pp. 19–26, 1970.
- [39] O. W. Holland, D. Fathy, and J. Narayan, "Dose rate effects in silicon during heavy ion irradiation," *Nucl. Instr. Meth. B*, vol. 10, no. 1, pp. 565–568, 1985.
- [40] J. R. Dennis, G. K. Woodward, and E. B. Hale, "Vacancy motion in ion-implanted silicon," in *Lattice Defects in Semiconductors*. London: Institute of Physics, 1975, pp. 467–473.
- [41] J. R. Dennis and E. B. Hale, "Crystalline to amorphous transformation in ion-implanted silicon: A composite model," *J. Appl. Phys.*, vol. 49, no. 3, pp. 1119–1127, 1978.
- [42] J. F. Gibbons, "Ion implantation in semiconductors—Part II: Damage production and annealing," *Proc. IEEE*, vol. 60, no. 9, pp. 1062–1096, 1972.
- [43] S. Mader, "Ion implantation damage in silicon," in *Ion Implantation: Science and Technology*, J. F. Ziegler, Ed. Orlando, FL: Academic, 1984, pp. 63–92.
- [44] M. Posselt and J. P. Biersack, "Influence of recoil transport on energy-loss and damage profiles," *Nucl. Instr. Meth. B*, vol. 15, pp. 20–24, 1986.
- [45] G. Bai and M.-A. Nicolet, "Defect production in Si(100) by  $^{19}\text{F}$ ,  $^{28}\text{Si}$ ,  $^{40}\text{Ar}$ , and  $^{131}\text{Xe}$  implantation at room temperature," *J. Appl. Phys.*, vol. 70, no. 7, pp. 3551–3555, 1991.

- [46] M. Jaraíz, J. Arias, J. E. Rubio, L. A. Bailón, and J. J. Barbolla, "Computer simulation of point-defect distributions generated by ion implantation," *Nucl. Instr. Meth. B*, vols. 80/81, pp. 172–175, 1993.
- [47] M. Jaraíz, J. Arias, E. Rubio, L. A. Marqués, L. Pelaz, L. Bailón, and J. Barbolla, "Dechanneling by thermal vibrations in silicon ion implantation," in *Proc. 10th Int. Conf. Ion Implantation Technology*, Catania, Italy, 1994, p. 2.19.
- [48] H. Serva and G. Hobler, "Comparison of transmission electron microscope cross sections of amorphous regions in ion implanted silicon with point defect density calculations," *J. Electrochem. Soc.*, vol. 139, pp. 3631–3638, 1992.
- [49] L. T. Chadderton, "Nucleation of damage centres during ion implantation of silicon," *Rad. Eff.*, vol. 8, nos. 1–2, pp. 77–86, 1971.
- [50] G. Carter, "The effects of flux, fluence and temperature on amorphization in ion implanted semiconductors," *J. Appl. Phys.*, vol. 79, no. 11, pp. 8285–8289, 1996.



**Walter Bohmayr** was born in Steyr, Austria, in 1969. He received the Dipl.-Ing. degree in control theory and industrial electronics from the Vienna University of Technology, Austria, in 1993. He received the Dr.techn. degree (*summa cum laude*) from the Institute for Microelectronics, Vienna University of Technology, in 1996.

He held a visiting research position with the Atsugi Technology Center, Sony Corp., Japan. Since 1997, he has been with ISE Integrated Systems Engineering AG, Zurich, Switzerland, where he is

in charge of the process simulation group. His work is focused on physical and mathematical models and algorithms for three-dimensional process simulation in integrated-circuit fabrication.

Dr. Bohmayr received the Award of the Federal Minister of Science and Research in 1994 and 1997. In 1995, the SUSTAIN Coordination Board awarded him the SUSTAIN fellowship at the Fraunhofer Institute of Integrated Circuits, Erlangen, Germany. He was honored by the federal president (*Promotio sub auspiciis Praesidentis rei publicae*).



**Alexander Burenkov** received the Dipl.-Phys. degree from the Technical University of Dresden, Germany, in 1974, the Cand.Sc. degree from the University of Rostov, Russia, in 1981, and the Dr.Sc. (VAK Moscow) from the Byelorussian State University, Minsk, Belarus, in 1991.

From 1974 to 1991, he was with the Institute of Applied Physics, Byelorussian State University, where he worked in the areas of ion implantation, ion-beam analysis, and technology. In 1983–1984, he received a fellowship from the Danish Ministry

of education and took part in an international project investigating passage of the fast GeV-particles through thin semiconductor layers. From 1991 to 1994, he was with Silvaco Data Systems GmbH, Munich, Germany. Since 1994, he has been with the Fraunhofer Institute of Integrated Circuits, Erlangen, Germany. He is the author or coauthor of three books and more than 80 papers in the field of ion-beam physics and technology. His present research area is simulation of CMOS technology, especially of ion implantation and software development for technology modeling in microelectronics.



**Jürgen Lorenz** received the Dipl.-Phys. and Dipl.-Math. degrees from the Technical University, Munich, Germany, in 1982 and 1984, respectively.

Having joined FhG in 1983, he moved in 1985 to the newly founded Fraunhofer Institute of Integrated Circuits, Erlangen, Germany, where since then he has been in charge of the Technology Simulation Department. His present research areas are the development of process models and simulation software in two and especially in three dimensions.

He is the author or coauthor of more than 70 papers and has been responsible for various research projects in these fields, including the PROMPT/PROMPT II projects on the development of a program system for multidimensional/three-dimensional process simulation.



**Heiner Ryssel** received the Dipl.-Ing. and Dr.-Ing. degrees in electrical engineering from the Technical University, Munich, Germany, in 1967 and 1973, respectively.

From 1968 to 1972, he was with the Institute of Technical Electronics, working on GaAs epitaxy and ion implantation. In 1973, he joined the Institute of Integrated Circuits, where he worked on ion implantation in Si, Ge, and III–V compounds. In 1974, he joined the Institute of Solid State Technology, Munich, where he worked in the area of semiconductor

device development and basic implantation studies. Since 1985, he has been a Professor of electrical engineering at the University of Erlangen-Nuremberg, Germany, and Director of the Fraunhofer Institute of Integrated Circuits, Erlangen. His main research topics are ion implantation into semiconductors and metals, process modeling, and semiconductor processing equipment.

**Siegfried Selberherr** (M'79–SM'84–F'93), for a photograph and biography, see p. 572 of the July 1998 issue of this TRANSACTIONS.